doi.org/10.36721/PJPS.2026.39.10.293.1

Exploration of the antagonistic action of BVP on TBHP induced apoptosis of primary rat retinal ganglion cells

Xiaoyong Huang[1] and Peng Chen[2]*

[1]Department of Neurology, Haian People's Hospital, Haian, Jiangsu, 226600, China
[2]Department of Neurology, The Sixth People's Hospital of Nantong, Nantong, Jiangsu, 226003, China

Abstract: **Background**: Oxidative stress-induced retinal ganglion cell (RGC) apoptosis is a common pathological pathway in optic neuropathies. Breviscapine (BVP) possesses antioxidant properties, but its protective effect against RGC apoptosis remains unclear. **Objectives**: To investigate the antagonistic effect of BVP on tert-butyl hydroperoxide (TBHP)-induced apoptosis in primary rat RGCs and evaluate its dose-dependency. **Methods**: Primary RGCs from 10 Sprague-Dawley (SD) rats were exposed to TBHP (100 μmol/L) and treated with BVP (0, 10, 20, 50 μmol/L). Apoptosis was assessed by terminal deoxynucleotidyl transferase dUTP nick end labeling (TUNEL) and Annexin V/propidium iodide (Annexin V/PI) flow cytometry. Protein expression of synaptophysin, B-cell lymphoma-2 (Bcl-2), Bcl-2-associated X protein (Bax) and cleaved caspase-3 was measured by Western blotting. **Results**: BVP treatment significantly increased synaptophysin and Bcl-2 expression, decreased Bax and cleaved caspase-3 expression and reduced the apoptotic rate in a dose-dependent manner ($P < 0.05$). The apoptotic rates in the blank control, disease control, low-dose, medium-dose and high-dose BVP groups were (2.12 ± 0.73)%, (64.13 ± 10.14)%, (14.13 ± 4.12)%, (10.23 ± 3.03)% and (6.13 ± 3.12)%, respectively. Flow cytometry confirmed that the total apoptotic rate in the high-dose group decreased to (5.79 ± 0.89)%, approaching the level of the blank control group. **Conclusion**: BVP inhibits TBHP-induced RGC apoptosis in a dose-dependent manner, possibly by regulating the Bcl-2/Bax/caspase-3 pathway. These findings support its potential as a therapeutic candidate for oxidative stress-associated optic neuropathies.

Keywords: Breviscapine; Cell apoptosis; Tetinal ganglion cells; Tert-butyl hydroperoxide

Submitted on 16-01-2026 – Revised on 09-05-2026 – Accepted on 21-05-2026

INTRODUCTION

Glaucoma is a common ophthalmic disease characterized by decreased visual acuity and abnormally elevated intraocular pressure (IOP) (Kashaf *et al*., 2026). Oxidative stress is a key factor in the development and progression of chronic eye diseases, including glaucoma. Ocular tissue is chronically exposed to ultraviolet radiation, leading to increased production of reactive oxygen species (ROS). Elevated ROS levels cause trabecular meshwork changes, elevate IOP, damage mitochondria and promote RGC apoptosis (Rejas-Gonzalez *et al*., 2024). Breviscapine (BVP) is a natural flavonoid compound extracted from *Erigeron breviscapus*, a medicinal plant widely used in traditional Chinese medicine. BVP possesses multiple pharmacological activities, including vasodilation, improved microcirculation, anti-inflammatory effects, and antioxidant properties. Clinically, BVP has been widely used to treat cardiovascular and cerebrovascular diseases (Lan *et al*., 2022). Tert-butyl hydroperoxide (TBHP) is an organic peroxide that can be metabolized by cytochrome P450 in cells to produce peroxy and alkoxy radicals or be detoxified to tert-butanol (Azeredo *et al*., 2025). TBHP can irritate the eyes and skin following inhalation, oral administration, or skin absorption (Ulagesan *et al*., 2023). Related studies have established a TBHP-induced optic nerve injury model in rats and treated the animals with BVP (Sun *et al*., 2023). Their findings revealed that compared with the control group, apoptosis-related proteins and neural marker proteins in the disease control group were significantly decreased. Compared with the disease control group, apoptotic cells in the BVP treatment group were significantly decreased, while apoptosis-related proteins and neural marker proteins were significantly increased, indicating that BVP protects against optic nerve cell apoptosis. However, whether BVP protects RGCs from TBHP-induced oxidative stress-mediated apoptosis and whether this effect is dose-dependent remain unclear. This study aimed to investigate the antagonistic effect of BVP on TBHP-induced RGC apoptosis and its dose-dependency.

MATERIALS AND METHODS

Experimental design

This study consisted of two independent sub-experiments. Sub-experiment 1 (*in-vitro*): To investigate the protective effect and dose-dependency of BVP against TBHP-induced oxidative stress injury in RGCs. Ten healthy male SD rats (2 months old) were sacrificed and their retinas were isolated for primary RGC culture. Cells were injured with TBHP (100 μmol/L) and then treated with low, medium and high doses of BVP (10, 20 and 50 μmol/L). Apoptosis rates, apoptosis-related proteins and neural

**Corresponding author:* e-mail: nchenyong333@163.com

marker proteins were measured. Sub-experiment 2 (*in-vivo*): To investigate the effect of BVP on IOP and retinal structure in a rat model of ocular hypertension. Another 50 healthy male SD rats (20-22 months old) were randomly divided into a blank control group (n=10), a disease control group (n=10), and BVP treatment groups (n=30, with low-, medium-, and high-dose groups of 10 rats each). The experimental workflow is shown in fig. 1. An ocular hypertension model was established by cauterizing the episcleral veins. After surgery, different doses of BVP or normal saline were administered by intragastric gavage. IOP, retinal thickness and optic nerve ultrastructure were measured.Rationale for experimental design: Sub-experiment 1 verified the direct protective effect of BVP against oxidative stress-induced RGC apoptosis *in-vitro*. Sub-experiment 2 verified the comprehensive therapeutic effect of BVP in an ocular hypertension model, whose pathological mechanism involves multiple factors, including oxidative stress, ischemia and hypoxia. The two sub-experiments complement each other and together provide experimental evidence for the use of BVP in treating oxidative stress-associated optic neuropathies, including glaucoma.

Experimental animals

Healthy male SD rats were provided by Changsha Tianqin Biotechnology Co., Ltd. [License No.: SCXK (Wan) 2003-007]. Sub-experiment 1 (*in-vitro*): Ten 2-month-old SD rats (body weight 200-250 g) were used for primary RGC isolation and culture.Sub-experiment 2 (*in-vivo*): Another 50 SD rats aged 20-22 months (body weight 400-450 g) were randomly divided into 5 groups of 10 rats each: blank control group, disease control group, low-dose group, medium-dose group and high-dose group.The specific treatments for each group were as follows:Blank control group: Intragastric administration of normal saline once daily for 8 consecutive weeks.Disease control group: Ocular hypertension model established (see section 2.6), followed by intragastric administration of normal saline once daily for 8 consecutive weeks.Low-dose group: Ocular hypertension model established, followed by intragastric administration of BVP (Approval No.: Z13020778, Manufacturer: Shenwei Pharmaceutical Group Co., Ltd.) at 0.025 mg/kg (equivalent to the *in-vitro* dose of 10 μmol/L) once daily for 8 consecutive weeks.Medium-dose group: Ocular hypertension model established, followed by intragastric administration of BVP at 0.05 mg/kg (equivalent to the *in-vitro* dose of 20 μmol/L) once daily for 8 consecutive weeks.High-dose group: Ocular hypertension model established, followed by intragastric administration of BVP at 0.125 mg/kg (equivalent to the *in-vitro* dose of 50 μmol/L) once daily for 8 consecutive weeks.

The administration volume was 0.5 mL per rat and the drug was prepared in normal saline. At 24 hours after the last administration, rats were deeply anesthetized with intraperitoneal pentobarbital sodium (40 mg/kg) and then euthanized by cervical dislocation. After weighing, the rats were placed in a beaker with 75% alcohol for disinfection and dissection. The cornea was cut along the corneoscleral margin and the retina was separated.

Cell culture and model preparation

Cell isolation and culture: Ten SD rats from Sub-experiment 1 were anesthetized and sacrificed and both eyeballs were removed. The eyeballs were incised along the corneal limbus and the retinal tissue was isolated. The retinal tissue was rinsed with DMEM (Shanghai Yuchun Biotechnology Co., Ltd.), minced, and then incubated with 1 mL of 0.25% trypsin (Shanghai Xinyu Biotechnology Co., Ltd.) at 37°C in a 5% CO_2 incubator for 15 minutes. Digestion was terminated by adding DMEM containing 10% fetal bovine serum (FBS). The cells were dispersed by pipetting, filtered through a 200-mesh filter and seeded at a density of 1×10^8 cells/mL into polylysine-coated 6-well plates. The cells were cultured in a 37°C, 5% CO_2 incubator. The medium was changed every 3 days and the cells were used for experiments after 7 days of culture.TBHP injury model establishment: According to a method from the literature, TBHP (Jinan Zhiding Trading Co., Ltd.) was added to the cell culture medium at a final concentration of 100 μmol/L. Incubation was continued for 24 hours to induce oxidative stress injury in RGCs.

Immunofluorescence staining

Isolated RGCs were plated on glass coverslips and treated with 20 μmol/L BVP. The culture medium was aspirated and cells were rinsed with phosphate-buffered saline (PBS) three times for 5 minutes each, then fixed with 4% paraformaldehyde. Cell membranes were permeabilized with PBS containing 0.1% Triton X-100. Cells were blocked with bovine serum albumin (BSA) solution and then incubated with primary antibodies overnight at 4°C. Cells were rinsed with PBS three times for 5 minutes each, incubated with secondary antibodies for 1 hour at room temperature and rinsed again with PBS. Coverslips were mounted onto glass slides with mounting medium containing DAPI and photographed using a fluorescence microscope (Shindler *et al*., 2023).

Western blotting assay

RGCs were seeded into 6-well plates, pretreated with 20 μmol/L BVP and then incubated with 100 μmol/L TBHP. Cells were collected using cell lysis buffer. The cytoplasm (without mitochondria and nuclei) was separated according to the kit instructions. Protein concentration was quantified using the bicinchoninic acid (BCA) method and 10 μg of protein was loaded per well. Proteins were separated by SDS-polyacrylamide gel electrophoresis and transferred to nitrocellulose membranes.

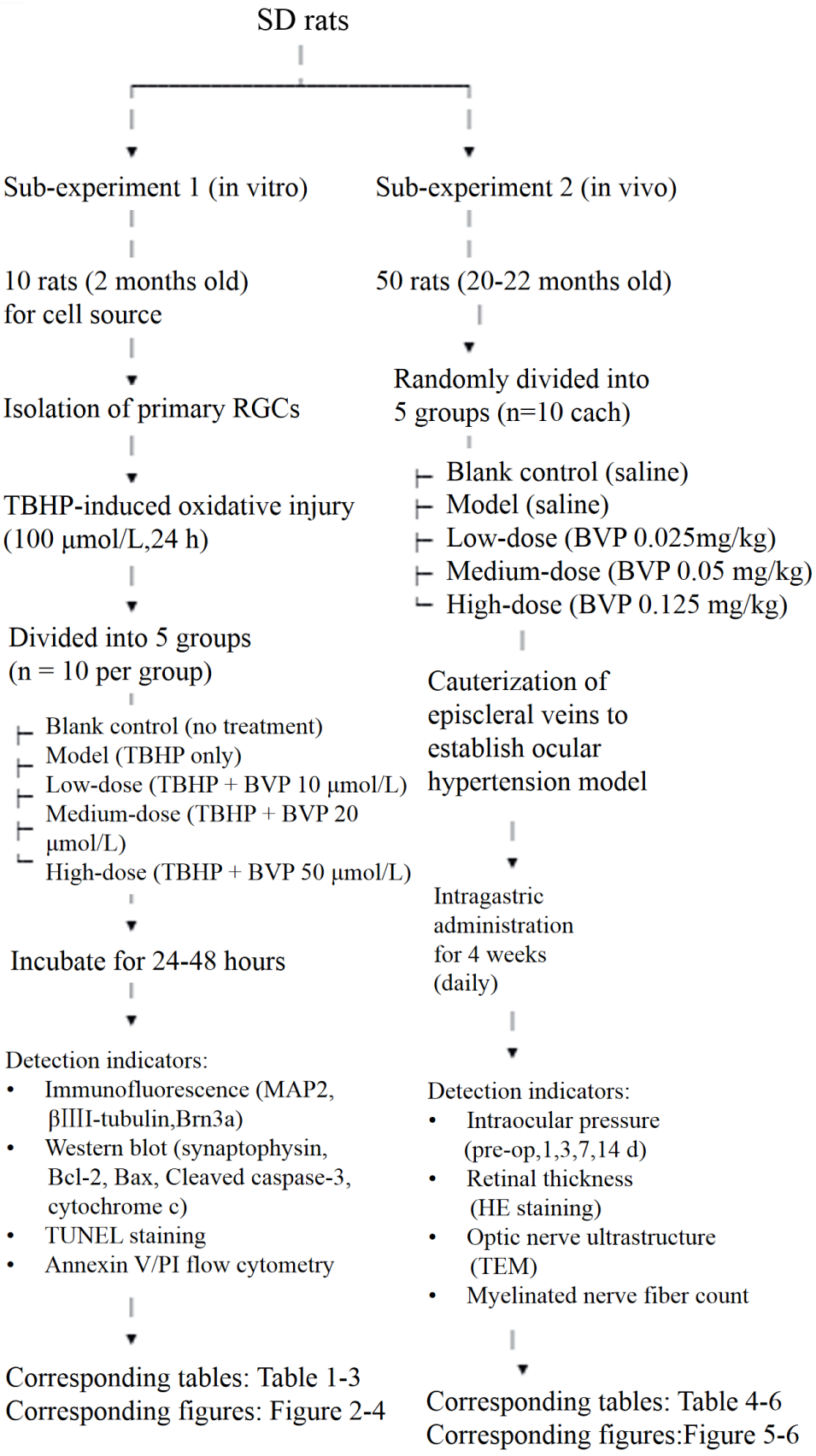

Fig. 1: Experimental design flowchart of this study.

Membranes were blocked with 5% non-fat milk in Tris-buffered saline with Tween (TBST) for 1 hour at room temperature, then incubated with primary antibodies against synaptophysin, Bcl-2, Bax and cleaved caspase-3 overnight at 4°C. After washing three times with TBST, membranes were incubated with horseradish peroxidase (HRP)-conjugated secondary antibodies for 1 hour at room temperature. Protein bands were visualized using an enhanced chemiluminescence (ECL) detection system and quantified using ImageJ software (McElhinney *et al*., 2024).

Detection of apoptosis rate of RGCs

TUNEL assay: Apoptosis was measured using a TUNEL Cell Apoptosis Detection Kit. Cells were fixed with 4% paraformaldehyde and then post-fixed with ethanol-acetic acid solution. Equilibrium solution and working solution were added for incubation. Stop buffer and fluorescent antibody dilution buffer were added and cells were counterstained with DAPI. Sections were sealed and staining results were observed under a fluorescence microscope. The percentage of TUNEL-positive cells was calculated as the apoptosis rate.

Annexin V/PI flow cytometry (Liu *et al*., 2024a): Apoptosis was also detected using an Annexin V-FITC/PI Apoptosis Detection Kit (Beyotime Biotechnology, Nantong, China, Catalog No.: C1062M). After treatment, cells from each group were digested with 0.25% trypsin without EDTA, centrifuged at 1000 rpm for 5 minutes and the cell pellet was collected. Cells were washed twice with pre-chilled PBS, resuspended in 500 μL of 1× Binding Buffer and adjusted to a density of 1 × 10^8cells/mL. Then, 100 μL of cell suspension (containing 1 × 10 ^5 cells) was mixed with 5 μL of Annexin V-FITC and 5 μL of PI, gently mixed, and incubated for 15 minutes at room temperature in the dark. After adding 400 μL of 1× Binding Buffer, samples were analyzed within 1 hour using a flow cytometer (BD FACSCalibur, USA). Data were analyzed using FlowJo software. Three replicates were performed per group and the experiment was independently repeated three times. The early apoptotic rate was defined as the percentage of Annexin V^+/PI^- cells and the total apoptotic rate was defined as the percentage of (Annexin V^+/PI^- + Annexin V^+/PI^+) cells.

Establishment of the ocular hypertension model and administration protocol

Ocular hypertension model establishment: Fifty SD rats from Sub-experiment 2 (10 per group) were acclimated for 1 week. Except for the blank control group, the remaining 40 rats were used to establish the ocular hypertension model according to a method from the literature (Lee *et al*., 2022). Rats were anesthetized with an intraperitoneal injection of 10% chloral hydrate at 3 mL/kg. The left eye was topically anesthetized with proparacaine eye drops (Suzhou Industrial Park Tianlong Pharmaceutical Co., Ltd., Approval No.: H20084062). Under a surgical microscope, a conjunctival incision was made in the superotemporal quadrant along the corneoscleral limbus, the scleral surface was exposed and the episcleral veins (temporal, superotemporal and subtemporal) were separated and cauterized. Antibiotic eye ointment was applied postoperatively to prevent infection. Rats in the blank control group underwent conjunctival incision followed by immediate suturing without cauterization. One week after surgery, IOP was measured using a Tono-pen II tonometer (Reichert, USA). IOP persistently above 22 mmHg was considered indicative of successful model establishment (Chen *et al*., 2025). The model success rate was 92% (37/40). Animals that failed were excluded and promptly replaced to ensure a final effective sample size of 10 rats per group.

Administration protocol: Starting from day 1 after surgery, rats in each treatment group received intragastric administration of BVP once daily for 4 weeks: low-dose group, 0.025 mg/kg; medium-dose group, 0.05 mg/kg; high-dose group, 0.125 mg/kg. The blank control and disease control groups received intragastric administration of an equal volume of normal saline. The administration volume was 0.5 mL per rat.

Intraocular pressure measurement: IOP was measured before surgery and at 1, 3, 7 and 14 days after surgery in each group of rats (10 rats per group). Proparacaine eye drops were used for topical anesthesia before measurement. IOP was measured three times per eye using a Tono-pen II tonometer (Reichert, USA) and the average value was recorded as the final IOP.

Retinal thickness measurement

After IOP measurement, rats were sacrificed. The left eyeball was removed and fixed with 4% paraformaldehyde for 24 hours, then dehydrated through a graded ethanol series and embedded in paraffin. Serial sections of 4 μm thickness were cut centered on the optic nerve and stained with hematoxylin and eosin (HE) (Nanchang Yulu Experimental Equipment Co., Ltd.) (Huan *et al*., 2023). Sections were observed and photographed under a light microscope. Retinal thickness (the distance from the inner limiting membrane to the outer limiting membrane) was measured using Image Pro Plus image analysis software. Five random fields were selected per section and the average value was taken as the retinal thickness for that sample.

Electron microscopy of optic nerve ultrastructure

After sacrifice, the optic nerve was quickly removed and fixed in 2.5% glutaraldehyde at 4°C overnight. After post-fixation with 1% osmium tetroxide, dehydration through a graded acetone series and embedding in epoxy resin, ultrathin sections (70 nm) were cut. Sections were double-

stained with uranyl acetate and lead citrate and then observed under a transmission electron microscope (Hitachi H-7650, Japan) to visualize optic nerve ultrastructure. Five random fields were selected per section (×60,000) and myelinated nerve fibers were counted. The average value was taken as the count for that sample (unit: per 100 μm²).

Statistical analysis

Sample size estimation: G*Power 3.1 was used. A significance level of $\alpha = 0.05$ (two-sided) and a power of $1-\beta = 0.80$ were set. Based on preliminary experimental results (effect size: Cohen's $d = 1.2$, $f = 0.5$), the required sample sizes per group were calculated to be 6 data points for *in-vitro* experiments and 8 animals for *in-vivo* experiments. Considering a 20% attrition rate (surgical failure, animal death, etc.), the final sample size was set to 10 per group for *in-vivo* experiments and a cumulative total of 10 data points per group (derived from 3 independent experiments) for *in-vitro* experiments.Normality and homogeneity tests: All continuous variables were first assessed for normality using the Shapiro-Wilk test (for sample sizes < 50). If the data followed a normal distribution ($P > 0.05$), parametric tests were used; otherwise, non-parametric tests were used. Homogeneity of variances was assessed using Levene's test. Multiple comparisons: For normally distributed data with homogeneous variances, a one-way analysis of variance (ANOVA) was used, followed by Tukey's HSD test (with adjustment for multiple comparisons). For data that were normally distributed but with unequal variances, Welch's ANOVA was used, followed by the Games-Howell test. For data that were not normally distributed, the Kruskal-Wallis H test was used, followed by Dunn's test with Bonferroni correction.Two-group comparisons: The independent samples t-test (for normally distributed data) or the Mann-Whitney U test (for non-normally distributed data) was used.Correlation analysis: Pearson's correlation was used for normally distributed data, and Spearman's rank correlation for non-normally distributed data.A P value < 0.05 (two-sided) was considered statistically significant. All multiple comparisons were adjusted using Tukey or Bonferroni methods. Statistical analysis was performed using SPSS 20.0 and graphs were created using GraphPad Prism 8.0.

BVP dose selection rationale.*In-vitro* doses: Preliminary experimental results showed that treating TBHP-injured RGCs with BVP at concentrations of 10-50 μmol/L for 24 hours increased cell viability in a dose-dependent manner.Studies by Sun et al. reported that BVP at concentrations of 50-100 μmol/L significantly inhibited cell apoptosis in a high glucose-induced podocyte injury model (Sun *et al*., 2023). Based on these preliminary experiments and literature results, concentrations of 10, 20, and 50 μmol/L were selected as the low, medium, and high doses for in *vitro* experiments.*In-vivo* doses: According to the body surface area conversion method recommended by the Food and Drug Administration (FDA), the *in-vitro* medium dose (20 μmol/L) was converted to an equivalent intragastric dose in rats of approximately 0.05 mg/kg. Additionally, the literature reports that intragastric administration of BVP at 15-30 mg/kg was safe and effective in mice, and, after interspecies conversion, the equivalent rat dose was approximately 7.5-15 mg/kg. Because this study used an acute oxidative stress injury model and RGCs may be more sensitive to BVP and given that preliminary experiments confirmed that the dose range of 0.025-0.125 mg/kg clearly demonstrated a dose-dependent protective effect, the low, medium and high doses for *in-vivo* experiments were set at 0.025, 0.05 and 0.125 mg/kg, respectively.

RESULTS

Identification of RGCs

Immunofluorescence staining was used to detect the expression of the RGC marker proteins MAP2, βIII-tubulin and Brn3a. The results showed that cultured cells stained positively for all three markers (Fig. 2), confirming that the cultured cells were RGCs.

Protective effects of different BVP doses on TBHP-injured RGCs

Western blotting results (Figs. 3 and 4 and Table 1) showed that, compared with the blank control group, synaptophysin expression was significantly decreased in the disease control group ($P < 0.05$). Compared with the disease control group, BVP treatment groups showed dose-dependent increases in synaptophysin expression ($P < 0.05$). Furthermore, Bcl-2, Bax and cleaved caspase-3 expression also showed dose-dependent changes (Table 2).

Effect of BVP on TBHP-induced RGC apoptosis

TUNEL staining and Annexin V/PI flow cytometry results (Fig. 5, Table 3) showed that the apoptotic rate in the blank control group was (2.12 ± 0.73)%, which increased to (64.13 ± 10.14)% in the disease control group ($P < 0.05$). After BVP treatment, the apoptotic rate decreased dose-dependently: low-dose group (14.13 ± 4.12%), medium-dose group (10.23 ± 3.03%), and high-dose group (6.13 ± 3.12%), all of which were significantly different from the disease control group ($P < 0.05$). Annexin V/PI flow cytometry further confirmed these results (Figs. 5A, 5B), with the total apoptotic rate in the high-dose group decreasing to (5.79 ± 0.89)%, approaching the level of the blank control group.

Changes in intraocular pressure

As shown in table 4, compared with preoperative values, IOP at all postoperative time points was significantly higher ($P < 0.05$).

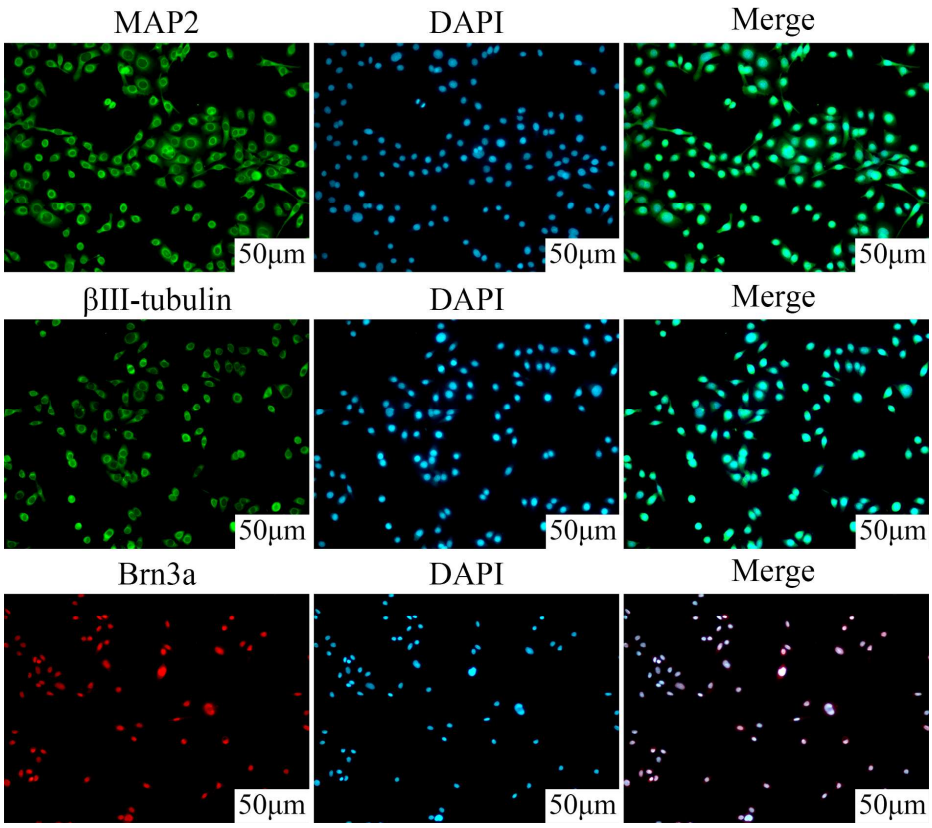

Fig. 2: Immunofluorescence staining (× 400).
A: MAP2 protein; B: βIII-tubulin; C: Brn3a protein.

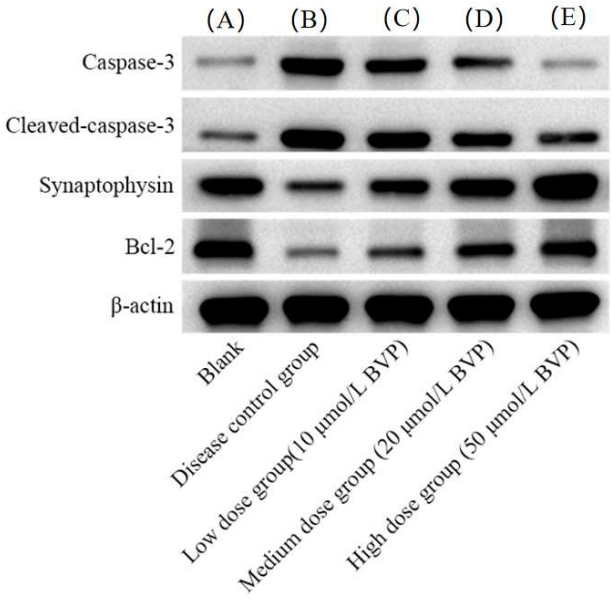

Fig. 3: Western blotting assay.
(A) Blank control group; (B) Disease control group (TBHP 100 μmol/L); (C) Low-dose BVP group (10 μmol/L); (D) Medium-dose BVP group (20 μmol/L); (E) High-dose BVP group (50 μmol/L). Protein bands shown are caspase-3, cleaved-caspase-3, synaptophysin, and Bcl-2. β-actin was used as a loading control.
BVP, breviscapine; RGCs, retinal ganglion cells; TBHP, tert-butyl hydroperoxide.

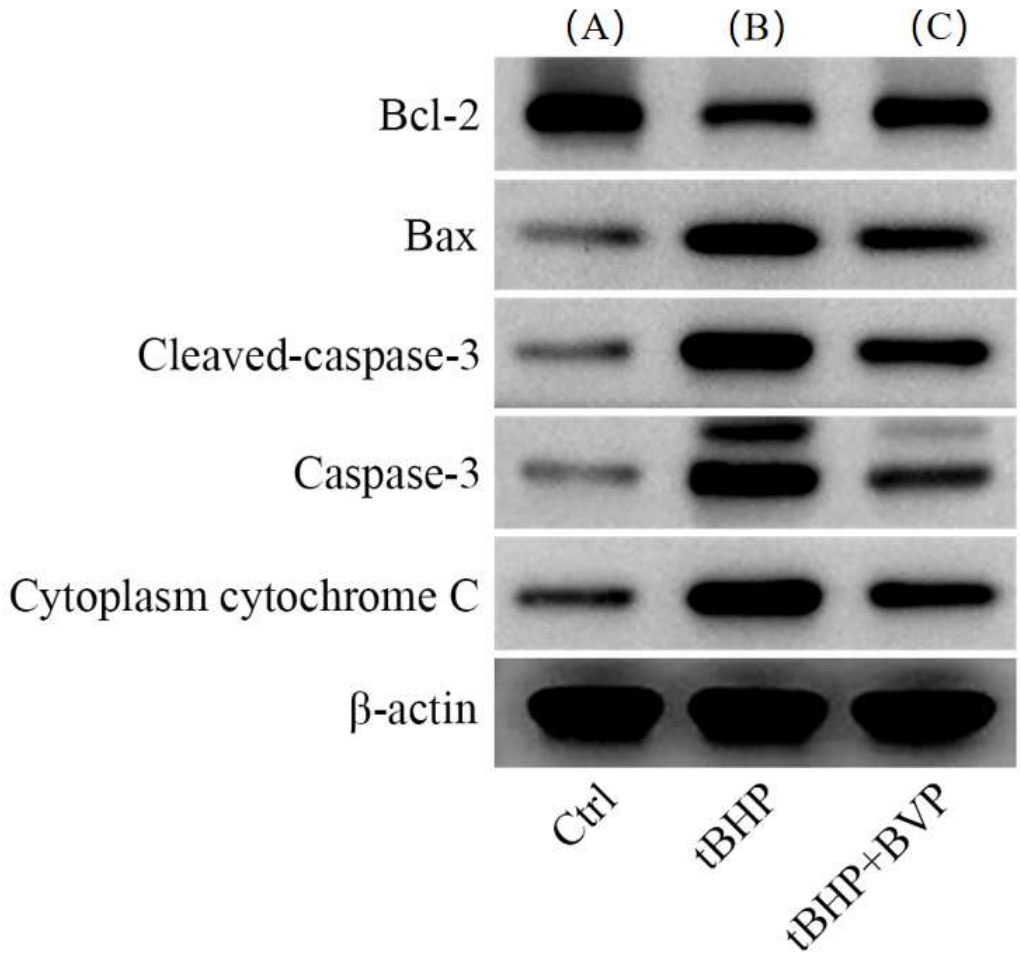

Fig. 4: Western blotting assay.
(A) Blank control group; (B) Disease control group (TBHP 100 μmol/L); (C) BVP treatment group (20 μmol/L).

Table 1: Relative expression levels of related neuroproteins in each group [($\bar{x} \pm s$),%].

Group	n	Caspase-3	Synatophysin	Cleaved-caspase-3	Bcl-2
Blank control group	10	100.01±10.42*	1.04±0.31*	1.04±0.01*	1.00±0.01
Disease control group	10	370.43±10.76	0.25±0.01	2.05±0.11	0.75±0.11
Low dose group(10 μmol/L BVP)	10	300.54±10.72	0.75±0.04	1.75±0.03	0.55±0.03
Medium dose group (20 μmol/L BVP)	10	150.53±9.65*	1.23±0.30*	1.53±0.20*	0.73±0.19
High dose group (50 μmol/L BVP)	10	100.45±9.23*	1.84±0.46*	1.24±0.26*	0.84±0.25

Note: *P < 0.05 vs. disease control group. Data were obtained from three independent experiments, with a cumulative total of 10 data points per group.

Table 2: Protective effect of BVP on TBHP induced apoptosis of rat optic nerve cells.

Group	Bcl-2	Cleaved-caspase-3	Bax	Cytoplasm cytochrome C	Mitochondrion cytochrome C
Blank control group	1.00±0.038	1.00±0.01*	1.00±0.02*	1.00±0.01*	1.00±0.03*
Disease control group	0.25±0.01	1.92±0.32	1.25±0.01	1.75±0.13	0.73±0.14
Treatment group (20 μmol/L BVP)	0.75±0.21*	1.22±0.12*	1.03±0.02*	1.12±0.04*	0.95±0.06*

Note: *P < 0.05 vs. disease control group.

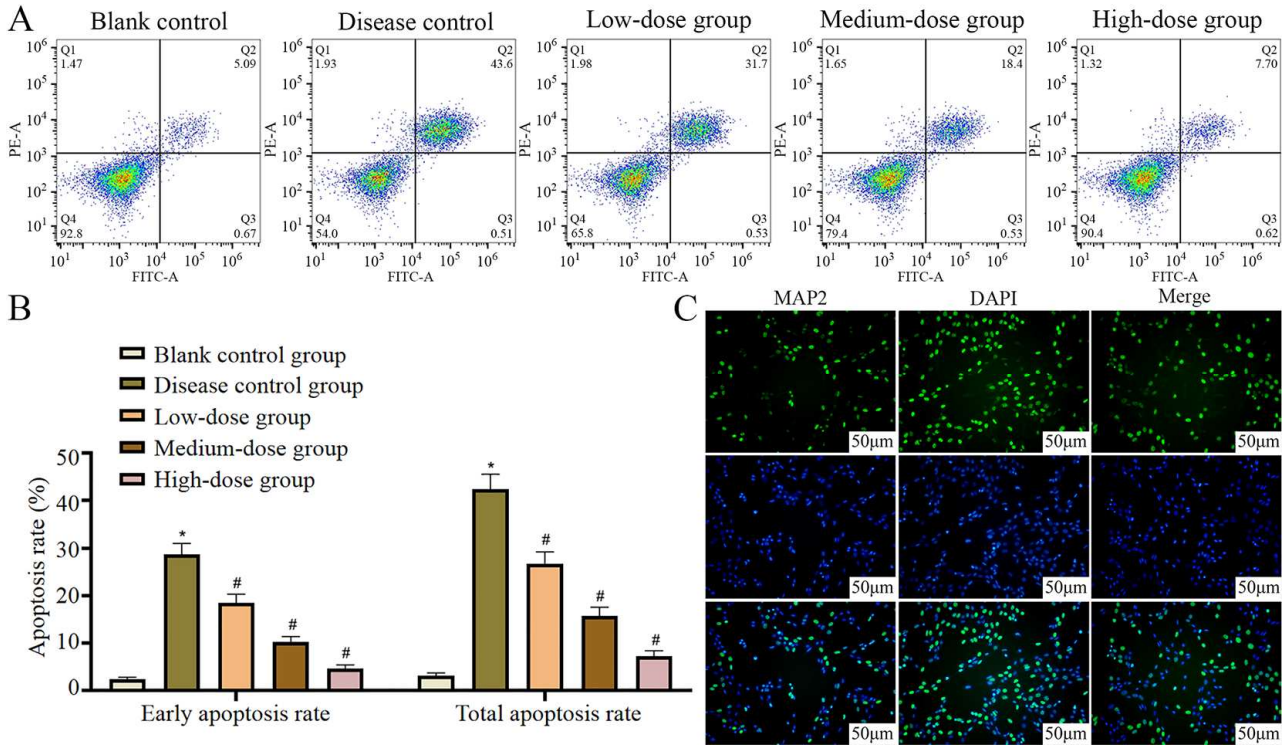

Fig. 5: Effect of different concentrations of BVP on TBHP-induced apoptosis of optic nerve cells.
(A) Representative Annexin V/PI dual-staining flow cytometry scatter plots; (B) Quantitative comparison of total apoptotic rate by Annexin V/PI flow cytometry. Data are presented as mean ± SD, n = 3 independent experiments; (C) Representative TUNEL staining images (×200). Scale bar = 100 μm. Data are presented as mean ± SD, n = 10.

Table 3: Comparison of apoptosis rate of optic nerve cells among various groups [($\bar{x} \pm s$),%].

Group	n	Apoptosis rate
Blank control group	10	2.12±0.73*
Disease control group	10	64.13±10.14
Low dose group(10 μmol/L BVP)	10	14.13±4.12*
Medium dose group (20 μmol/L BVP)	10	10.23±3.03*
High dose group (50 μmol/L BVP)	10	6.13±3.12*

Note: *P < 0.05 vs. disease control group.

Table 4: Changes in intraocular pressure in rats of each group [($\bar{x} \pm s$) mmHg].

Group	n	Before operation	1d after operation	3d after operation	7d after operation	14d after operation
Blank control group	10	12.68±0.95	12.28±1.12$^{\#}$	12.08±0.98$^{\#}$	12.08±1.05$^{\#}$	12.08±0.92$^{\#}$
Disease control group	10	12.16±0.87	32.48±2.65*	32.38±2.38*	32.58±2.22*	35.08±2.64*
Low-dose group (0.025 mg/kg)	10	12.38±0.91	32.95±2.10*	31.82±1.89*	30.05±2.11$^{*\#}$	28.61±2.27$^{*\#}$
Medium-dose group (0.05 mg/kg)	10	12.30±0.88	32.38±1.80*	29.28±1.72$^{*\#}$	25.18±1.65$^{*\#}$	18.30±1.40$^{*\#}$
High-dose group (0.125 mg/kg)	10	12.28±0.90	32.08±1.93*	27.08±1.65$^{*\#}$	22.08±1.79$^{*\#}$	12.08±0.52$^{\#}$

Note: *P < 0.05 vs. before operation; #P < 0.05 vs. disease control group. Intraocular pressure in the high-dose group returned to the level of the blank control group at 14 days postoperatively.

There was no significant difference in IOP among the groups before surgery (P > 0.05). There was no significant difference in IOP between the low- or medium-dose groups and the disease control group at 1, 3 and 7 days after surgery (P > 0.05), but postoperative IOP was significantly higher than that in the blank control group. However, at 14 days after surgery, IOP in the high-dose group was significantly lower than that in the disease control group (P < 0.05) and there was no significant difference between the high-dose group and the blank control group (P > 0.05).

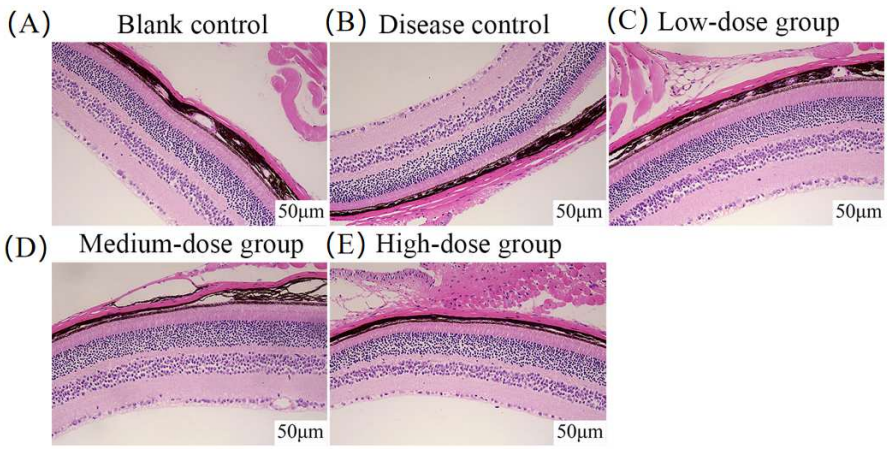

Fig. 6: Comparison of retinal thickness (HE×200).
(A) Blank control group: optic nerve fibers are densely and regularly arranged, with intact myelin sheaths and normal mitochondrial morphology; (B) Disease control group: optic nerve fibers are sparse, with disrupted myelin sheaths and deformed mitochondria; (C) Low-dose BVP group (0.025 mg/kg): mild improvement in fiber arrangement and myelin integrity compared with the disease control group, though the difference did not reach statistical significance ($P > 0.05$); (D) Medium-dose BVP group (0.05 mg/kg): moderate restoration of retinal thickness and myelin sheath structure; (E) High-dose BVP group (0.125 mg/kg): marked recovery of retinal thickness, approaching the level of the blank control group, with well-preserved myelin sheaths and mitochondrial morphology. Arrows indicate representative myelin sheath and mitochondrial structures. Scale bar = 50 μm.BVP, breviscapine; HE, hematoxylin and eosin.

Table 5: Comparison of retinal thickness in rats among various groups [($\bar{x} \pm s$)μm].

Group	n	Retinal thickness
Blank control group	10	193.28 ± 3.21^{b}
Disease control group	10	163.18 ± 2.52^{a}
Low-dose group (0.025 mg/kg)	10	166.42 ± 2.75^{ab}
Medium-dose group (0.05 mg/kg)	10	172.30 ± 2.60^{ab}
High-dose group (0.125 mg/kg)	10	178.10 ± 2.43^{ab}

Note: $aP < 0.05$ vs. blank control group; $bP < 0.05$ vs. disease control group. Retinal thickness recovery was most significant in the high-dose group.

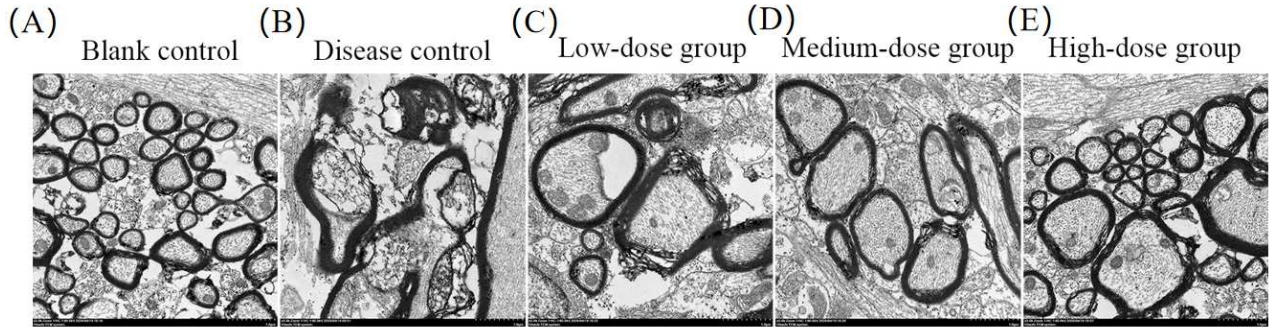

Fig. 7: Comparison of retinal thickness (× 60000).
(A) Blank control group: densely packed myelinated nerve fibers with intact myelin sheaths and normal mitochondrial cristae; (B) Disease control group: markedly reduced myelinated fiber density, with disrupted myelin lamellae and swollen/deformed mitochondria; (C) Low-dose BVP group (0.025 mg/kg): mild increase in myelinated fiber density, with residual myelin disruption; (D) Medium-dose BVP group (0.05 mg/kg): moderate improvement in myelin sheath integrity and mitochondrial morphology; (E) High-dose BVP group (0.125 mg/kg): substantial recovery of myelinated nerve fibers, with well-preserved myelin sheaths and mitochondrial structure, approaching the blank control level. Arrows indicate representative myelin sheath and mitochondrial structures. Scale bar = 50 μm.BVP, breviscapine.

Comparison of retinal thickness

HE staining results (Fig. 6, Table 5) showed that retinal thickness in the high-dose group (50 μmol/L BVP) was (178.14 ± 3.44) μm, which was significantly greater than that in the disease control group (163.21 ± 3.56 μm, $P < 0.05$) and showed no significant difference compared with the blank control group (193.32 ± 4.54 μm, $P > 0.05$). In contrast, retinal thickness in the low-dose group (166.45 ± 3.89 μm) did not reach statistical significance compared with the disease control group ($P > 0.05$). The medium-dose group (166.45 ± 3.89 μm) showed significant improvement compared with the disease control group ($P < 0.05$). These results indicate a dose-dependent protective effect of BVP.

Optic nerve ultrastructure and myelinated nerve fiber count

Transmission electron microscopy results (Fig. 7, Table 6) showed that in the blank control group, optic nerve fibers were densely and regularly arranged with intact myelin sheaths. In the disease control group, optic nerve fibers were sparse, with disrupted myelin sheaths and mitochondrial deformations. In the BVP treatment groups, these pathological changes were attenuated in a dose-dependent manner. Myelinated nerve fiber counts showed that the disease control group (53.32 ± 2.73 per 100 μm²) had significantly fewer fibers than the blank control group (93.32 ± 2.54 per 100 μm², $P < 0.05$). Compared with the disease control group, the high-dose BVP group (79.78 ± 2.94 per 100 μm²) showed the most significant recovery ($P < 0.05$), followed by the medium-dose group (70.42 ± 1.89 per 100 μm², $P < 0.05$) and the low-dose group (61.20 ± 2.11 per 100 μm², $P < 0.05$), demonstrating a dose-dependent protective effect of BVP (Table 6).

DISCUSSION

BVP, the main active component of Erigeron breviscapus, is a natural flavonoid compound that increases vascular flow, improves retinal blood circulation and inhibits blood coagulation (Niu *et al*., 2023).

In glaucoma patients, oxidative substances play an important role, injuring RGCs, glial cells, and trabecular meshwork cells, and potentially causing secondary injury (Hurley et al., 2022; Yang *et al*., 2024). During RGC apoptosis, mitochondrial cytochrome c is released into the cytoplasm, leading to caspase activation and, eventually, cell death (Zhao et al., 2023; Rajakrishna *et al*., 2025). The Bcl-2 protein has an anti-apoptotic effect. Various signal transduction pathways share a common regulatory point, the Bcl-2 protein (Aboelella *et al*., 2026).

In this study, treatment effects of different BVP concentrations on injured RGCs were observed. TBHP is an organic peroxide with good stability (Swenson *et al*., 2024). After TBHP treatment, RGC injury was successfully induced and synaptophysin expression was significantly decreased, consistent with the results of Ladakis *et al*. (2024). After BVP treatment, synaptophysin expression significantly increased, showing no significant difference from the blank control group and the treatment effect was dose-dependent. The apoptosis-related proteins Bcl-2, cleaved caspase-3 and Bax were examined. In the disease control group, Bax and cleaved caspase-3 expression levels were significantly increased, while Bcl-2 expression was significantly decreased, consistent with the results of Liu et al. (2024b). The present study found that BVP treatment increased Bcl-2 expression and decreased Bax and cleaved caspase-3 expression, suggesting that BVP may exert its anti-apoptotic effect by regulating the Bcl-2/Bax/caspase-3 signaling axis (Feng *et al*., 2022). However, this study is only a correlational observation and cannot determine whether Bcl-2 is the primary or sole pathway through which BVP exerts its protective effect. The Bcl-2 family protein regulatory network is complex and may interact with other signaling pathways (such as PI3K/Akt, MAPK). Subsequent studies should use pathway-specific inhibitors (such as the Bcl-2 inhibitor ABT-199) or genetic interventions (such as siRNA knockdown of Bcl-2 expression) to further verify the specific role of Bcl-2 in the anti-apoptotic effect of BVP.

To verify the effect of BVP on IOP, an ocular hypertension model was established using cauterization. The results showed that high-dose BVP (50 μmol/L) significantly reduced IOP in rats, bringing it to a level comparable to that of the blank control group by day 14 postoperatively. In contrast, IOP in the low-dose group remained elevated throughout the observation period ($P > 0.05$ vs. disease control group), suggesting that the ocular hypotensive effect of BVP is dose-dependent. The hypotensive mechanism may involve improving the function of the aqueous humor outflow channel, but the specific mechanism remains to be studied. In the study by Vitiello et al. (2023), BVP was reported to have a calcium antagonistic effect, protecting RGCs by inhibiting Ca^{2+} influx into smooth muscle cells. Calcium antagonists can inhibit calcium outflow and uptake, relax smooth muscle, inhibit vasodilation and improve aqueous humor flow (Ali *et al*., 2023). However, whether this mechanism participates in the IOP-lowering effect requires further experimental verification. In addition, the protective effect of BVP on injured RGCs was further demonstrated by retinal thickness measurements.

Oral gavage administration was chosen for this study primarily because the conventional dosage forms of BVP in clinical practice are oral preparations (tablets and capsules) and injections, which are mainly used to treat cardiovascular and cerebrovascular diseases. Oral administration is the most convenient and safe method for BVP in clinical practice.

Table 6: Number of myelinated nerve fibers in each group [($\bar{x} \pm s$), / 100μm^2].

Group	n	Number of myelinated nerve fibers
Blank control group	10	93.28±1.80[b]
Disease control group	10	53.30±1.93[a]
Low-dose group (0.025 mg/kg)	10	61.20±2.11[ab]
Medium-dose group (0.05 mg/kg)	10	70.42±1.89[ab]
High-dose group (0.125 mg/kg)	10	79.75±2.08[ab]

Note: *a* P < 0.05 vs. blank control group; *b* P < 0.05 vs. disease control group. The number of myelinated nerve fibers in the high-dose group showed the best recovery.

Furthermore, the *in-vivo* part of this study used an ocular hypertension model involving surgical manipulation of the eye. Topical eye drop administration in the early postoperative period might affect drug absorption due to ocular inflammation or corneal epithelial injury. Therefore, oral gavage ensured the accuracy and consistency of drug administration.

This study has the following limitations. (1) The TBHP model is an acute oxidative stress model and cannot fully simulate the chronic pathological process of human glaucoma. (2) Although changes in the Bcl-2/Bax/caspase-3 pathway were detected, pathway-specific inhibitors or genetic interventions were not used for verification; therefore, a causal relationship cannot be established. (3) Pharmacokinetic studies were not conducted and data on BVP distribution in ocular tissues are lacking. (4) The efficacy difference between oral and topical administration was not compared. (5) Long-term safety and the optimal therapeutic window were not evaluated. Therefore, the conclusions of this study cannot be directly extrapolated to clinical application. Subsequent studies should verify long-term efficacy in chronic animal models and conduct pharmacokinetic-pharmacodynamic studies to evaluate the potential for clinical translation.

CONCLUSION

In summary, BVP exhibits significant neuroprotective effects in both the TBHP-induced rat RGC oxidative stress injury model and the ocular hypertension model. Its mechanism may involve regulation of the Bcl-2/Bax/caspase-3 signaling pathway. These findings provide experimental evidence for preclinical studies of BVP in treating oxidative stress-associated optic neuropathies, but its clinical efficacy and safety require further research and validation.

Acknowledgments
We gratefully acknowledge the Haian People's Hospital for providing the necessary equipment for this study.

Authors' contributions
Xiaoyong Huang: Conceptualization, methodology, investigation, data curation and writing – original draft; Peng Chen: Project administration, resources, supervision, validation, writing – review and editing. All authors participated in data interpretation and manuscript revision and agreed to the submission and publication of the final version.

Funding
There was no funding.

Data availability statement
All data generated or analyzed during this study are included in this published article and its supplementary information files.

Ethical approval
All animal experiments were performed in strict accordance with the Guide for the Care and Use of Laboratory Animals and the ARRIVE guidelines. All measures were taken to minimize animal suffering. All surgical procedures were performed under anesthesia with intraperitoneal pentobarbital sodium (40 mg/kg). At the end of the experiments, rats were euthanized by cervical dislocation under deep anesthesia, a method that was reviewed and approved by the Ethics Committee of Haian People's Hospital (Approval No.: S2025-963). This study was performed in adherence with the ARRIVE guidelines. See supplementary file for the ARRIVE checklist.

Conflict of interest
The authors declare no conflict of interest.

Supplementary data
https://www.pjps.pk/uploads/2026/07/SUP1783856833.pdf

REFERENCES

Aboelella NS, Park R, Tang E, Asby N, Ho JD, Pan T, Wang S, Xie L, Kline JP, Riedell PA, Huang J and LaBelle JL (2026). Therapeutic targeting of BCL-2 during CART cell production augments potency through non-apoptotic adaptive changes. *Signal Transduct Target Ther*., **11**(1): 155.

Ali N, Ali W, Ullah A, Ahmad S, Alsaiari AA, Almehmadi M, Abdulaziz O, Allahyani M and Aljuaid A (2023). Atorvastatin and fluvastatin potentiate blood pressure lowering effect of amlodipine through vasorelaxant

phenomenon. *Medicina (Kaunas)*., **59**(6): 1023.

Azeredo PdS, Fix C, Pernomian L, Wenceslau CF, Piroli GG, Vicente CP and Carver WE (2025). Tetrahydrocurcumin outperforms curcumin in preventing oxidative stress-induced dysfunction in tert-butyl hydroperoxide-stimulated cardiac fibroblasts. *Int J Mol Sci*., **26**(13): 5964.

Chen L, Yan X, Luo Z, Cheng Y and Li M (2025). Vasoactive intestinal peptide reduces ocular hypertension by regulating tight junction of trabecular meshwork through Rab13/PKA signalling complex. *Ann Med*., **57**(1): 2534527.

Feng Y, Ju Y, Yan Z, Ji M, Yang M, Wu Q, Wang L and Sun G (2022). Protective role of wogonin following traumatic brain injury by reducing oxidative stress and apoptosis via the PI3K/Nrf2/HO-1 pathway. *Int J Mol Med*., **49**(4): 53.

Huan Y, Wu XQ, Chen T, Dou YN, Jia B, He X, Wei DY, Fei Z and Fei F (2023). Necroptosis plays a crucial role in the exacerbation of retinal injury after blunt ocular trauma. *Neural Regen Res*., **18**(4): 922-928.

Hurley DJ, Normile C, Irnaten M and O'Brien C (2022). The intertwined roles of oxidative stress and endoplasmic reticulum stress in glaucoma. *Antioxidants (Basel)*., **11**(5): 886.

Kashaf MS, Nagarajan N, Le JT, Rosman L, McCann P, E JY, Li T and Bicket AK (2026). A systematic review of patient-reported outcome instruments relevant to glaucoma. *J Glaucoma*., **35**(5): e15-e41.

Ladakis DC, Vreones M, Blommer J, Harrison KL, Smith MD, Vasileiou ES, Moussa H, Ahmadi G, Ezzedin O, DuVal AL, Dewey BE, Prince JL, Fitzgerald KC, Sotirchos ES, Saidha S, Calabresi PA, Kapogiannis D and Bhargava P (2024). Synaptic protein loss in extracellular vesicles reflects brain and retinal atrophy in people with multiple sclerosis. *Neurol Neuroimmunol Neuroinflamm*., **11**(4): e200257.

Lan T, Jiang S, Zhang J, Weng Q, Yu Y, Li H, Tian S, Ding X, Hu S, Yang Y, Wang W, Wang L, Luo D, Xiao X, Piao S, Zhu Q, Rong X and Guo J (2022). Breviscapine alleviates NASH by inhibiting TGF-β-activated kinase 1-dependent signaling. *Hepatology*., **76**(1): 155-171.

Lee KM, Song DY and Kim SH (2022). Effect of strain on rodent glaucoma models: Magnetic bead injection versus hydrogel injection versus circumlimbal suture. *Transl Vis Sci Technol*., **11**(9): 31.

Liu H, Ma L, Fu J, Ma X, Gao Y, Xie Y, Yuan X, Wang Y, Yang W and Jiang S (2024b). Effect of zearalenone on the jejunum of weaned gilts through the Epac1/Rap1/JNK pathway. *J Anim Sci*., **102**: skae208.

Liu J, Bao B, Li T, Yang Z, Du Y, Zhang R, Xin J, Hao J, Wang G, Bi H and Guo D (2024a). miR-92b-3p protects retinal tissues against DNA damage and apoptosis by targeting BTG2 in experimental myopia. *J Transl Med*., **22**(1): 511.

McElhinney K, Irnaten M, O'Callaghan J and O'Brien C (2024). p53 and the E3 Ubiquitin Ligase MDM2 in glaucomatous lamina cribrosa cells. *Int J Mol Sci*., **25**(22): 12173.

Niu P, Liu F, Lei F, Peng J, Wang Y, Zhao J, Gao Z, Gao Q and Gu J (2023). Breviscapine regulates the proliferation, migration, invasion and apoptosis of colorectal cancer cells via the PI3K/AKT pathway. *Sci Rep*., **13**(1): 9674.

Rajakrishna N, Lim ST, Wang X and Wong TT (2025). Caspase-mediated pathways in retinal ganglion cell injury: a novel therapeutic target for glaucoma. *Front Cell Dev Biol*., **13**: 1586240.

Rejas-González R, Montero-Calle A, Pastora Salvador N, Crespo Carballés MJ, Ausín-González E, Sánchez-Naves J, Pardo Calderón S, Barderas R and Guzman-Aranguez A (2024). Unraveling the nexus of oxidative stress, ocular diseases and small extracellular vesicles to identify novel glaucoma biomarkers through in-depth proteomics. *Redox Biol*., **77**: 103368.

Shindler RE, Yue J, Chaqour B, Shindler KS and Ross AG (2023). Repeat Brn3a immunolabeling rescues faded staining and improves detection of retinal ganglion cells. *Exp Eye Res*., **226**: 109310.

Sun L, Ding M, Chen F, Zhu D and Xie X (2023). Breviscapine alleviates podocyte injury by inhibiting NF-κB/NLRP3-mediated pyroptosis in diabetic nephropathy. *PeerJ*., **11**: e14826.

Swenson KA, Min K and Konopka JB (2024). *Candida albicans* pathways that protect against organic peroxides and lipid peroxidation. *PLoS Genet*., **20**(10): e1011455.

Ulagesan S, Krishnan S, Nam TJ and Choi YH (2023). Crassostrea gigas peptide PEP-1 prevents tert-butyl hydroperoxide (t-BHP) induced oxidative stress in HepG2 cells. *Food Sci Biotechnol*., **33**(5): 1245-1254.

Vitiello L, Capasso L, Cembalo G, De Pascale I, Imparato R and De Bernardo M (2023). Herbal and natural treatments for the management of the glaucoma: An update. *Biomed Res Int*., **2023**: 3105251.

Yang TH, Kang EY, Lin PH, Yu BB, Wang JH, Chen V and Wang NK (2024). Mitochondria in retinal ganglion cells: Unraveling the metabolic nexus and oxidative stress. *Int J Mol Sci*., **25**(16): 8626.

Zhao WJ, Fan CL, Hu XM, Ban XX, Wan H, He Y, Zhang Q and Xiong K (2023). Regulated cell death of retinal ganglion cells in glaucoma: Molecular insights and therapeutic potentials. *Cell Mol Neurobiol*., **43**(7): 3161-3178.